February 7, 2008

Search for light pseudoscalar sgoldstino in K^- decays

O.G. Tchikilev, S.A. Akimenko, G.I. Britvich, K.V. Datsko, A.P. Filin, A.V. Inyakin, V.A. Khmelnikov, A.S. Konstantinov, V.F. Konstantinov, I.Y. Korolkov, V.M. Leontiev, V.P. Novikov, V.F. Obraztsov, V.A. Polyakov, V.I. Romanovsky, V.I. Shelikhov, N.E. Smirnov, V.A. Uvarov, O.P. Yushchenko.

Institute for High Energy Physics, Protvino, Russia

V.N. Bolotov, S.V. Laptev, A.R. Pastsjak, A.Yu. Polyarush.

Institute for Nuclear Research Moscow, Russia

Abstract

A search for the light pseudoscalar sgoldstino production in the three-body K^- decay $K^- \to \pi^- \pi^0 \, P$ has been performed with the "ISTRA+" detector exposed to the 25 GeV/c negative secondary beam of the U-70 proton synchrotron. No signal is observed. An upper limit for the branching ratio $Br(K^- \to \pi^- \pi^0 P)$, at 90% confidence level, is determined to be $\sim 9 \cdot 10^{-6}$ in the effective mass m_P range from 0 to 200 MeV/c^2, excluding the region near m_{π° where it degrades to $\sim 3.5 \cdot 10^{-5}$.

1 Introduction

In models with spontaneous supersymmetry breaking the superpartners of a Goldstone fermion, pseudoscalar P and scalar S goldstinos, should exist. In some versions of gravity-mediated and gauge-mediated theories (for a recent review see [1]) one or both of these weakly interacting bosons (sgoldstinos) are light enough to be observed in kaon decays. Moreover, if sgoldstino interactions with quarks conserve parity, as in left-right extensions of MSSM, and P is lighter than S, so that $m_S > (m_K - m_\pi)$ and $m_P < (m_K - 2m_\pi)$, sgoldstinos can be observed in the decay $K \to \pi\pi P$(see Fig.1), rather than in the much better constrained $K \to \pi S$. The phenomenology of light sgoldstinos in this scenario is considered in detail in [2]. Under the assumption that sgoldstino interactions with quarks and gluons violate quark flavor and conserve parity, low energy interactions of pseudoscalar sgoldstino P with quarks are described by the Lagrangian:

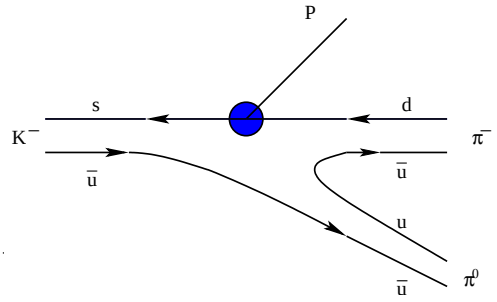

Figure 1: K^- decay into sgoldstino and pions.

$$L = -P \cdot (h^D_{ij} \cdot \overline{d}_i i\gamma^5 d_j + h^U_{ij} \cdot \overline{u}_i i\gamma^5 u_j) \,, \tag{1}$$

where

$$d_i = (d, s, b) \,, \qquad u_i = (u, c, t) \,,$$

and with coupling constants h_{ij} proportional to the left-right soft terms in the mass matrix of squarks:

$$h^D_{ij} = \frac{\tilde{\mathfrak{m}}^{(LR)2}_{D,ij}}{\sqrt{2}F} \,, \qquad h^U_{ij} = \frac{\tilde{\mathfrak{m}}^{(LR)2}_{U,ij}}{\sqrt{2}F} \,, \tag{2}$$

where the scale of supersymmetry breaking is denoted as $\sqrt{F}$.
The 90% confidence level (CL) constraints on the flavor-violating coupling of sgoldstinos to quarks evaluated using the $K^\circ_L - K^\circ_S$ mass difference and CP violating parameter ϵ in the neutral kaon system are: $|h^D_{12}| \leq 7 \cdot 10^{-8}$; $|\mathrm{Re}(h^D_{12})\mathrm{Im}(h^D_{12})| < 1.5 \cdot 10^{-17}$. It has been shown [2] that, depending on the phase of sgoldstino-quark coupling, these constraints result in the following 90% CL upper limits on the branching ratio: $Br(K^- \to \pi^-\pi^0 P) \leq 1.5 \cdot 10^{-6}$ — $4 \cdot 10^{-4}$, where the less strong limit corresponds to the case of pure real or pure imaginary h^D_{12} . A search for P in charged kaon decays is of particular interest when $\mathrm{Re}(h^D_{12}) \sim 0$, and when related branching ratio for the decay $K_L \to \pi^-\pi^+ P$ is small.

Light sgoldstinos decay into two photons or into a pair of charged leptons. The two photon decay dominates almost everywhere in the parameter space. Depending on the parameter $g_\gamma = \frac{1}{2\sqrt{2}}\frac{M_{\gamma\gamma}}{F}$, where $M_{\gamma\gamma}$ is the photino mass, sgoldstinos will have a very different lifetime. In the present search we assume that the sgoldstino is sufficiently long lived to decay outside the detector, i.e. the sgoldstino is "invisible". The existing 90% CL upper limit on the branching ratio $Br(K^- \to \pi^-\pi^0 P)$ is $4 \cdot 10^{-5}$ [3], whereas the 90% CL upper limits for the scalar sgoldstino S estimated from the studies of the $K^+ \to \pi^+\nu\overline{\nu}$ vary between $0.4 \cdot 10^{-10}$ and $1.0 \cdot 10^{-10}$ in the mass interval from 0 to 110 MeV/c^2,

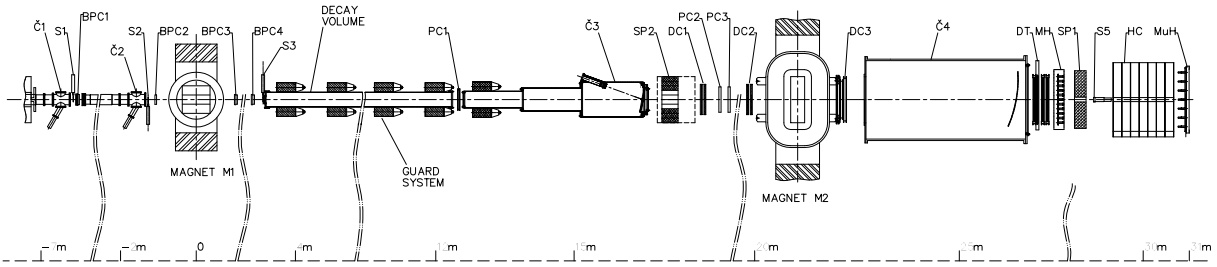

Figure 2: The elevation view of the ISTRA+ setup. M_1 and M_2 are magnets, $\check{C}_i$ — Cerenkov counters, BPC_i — beam proportional chambers, PC_i — spectrometer proportional chambers, SP_i — lead glass calorimeters, DC_i — drift chambers, DT_i — drift tubes, HC — a hadron calorimeter, S_i — trigger scintillation counters, MH — a scintillating hodoscope and MuH — a scintillating muon hodoscope.

see Fig. 3 in [6]). The recent upper limit for the decay $K^+ \to \pi^+ X^\circ$, where X° is a neutral weakly interacting massless particle, is $0.73 \cdot 10^{-10}(90\%$ CL)[5].

The aim of our present study is to search for invisible pseudoscalar sgoldstinos in the K^- decays. The experimental setup and event selection are described in section 2, the results of the analysis are presented in section 3, the systematic uncertainties are discussed in section 4 and the conclusions are given in the last section.

2 Experimental setup and event selection

The experiment is performed at the IHEP 70 GeV proton synchrotron U-70. The ISTRA+ spectrometer has been described in some detail in our recent papers on K_{e3} [7], $K_{\mu 3}$ [8] and $\pi^-\pi^\circ\pi^\circ$ decays [9]. Here we recall briefly the characteristics relevant to our analysis. The ISTRA+ setup is located in a negative unseparated secondary beam line 4A of U-70. The beam momentum is ~ 25 GeV/c with $\Delta p/p \sim 1.5\%$. The admixture of K^- in the beam is $\sim 3\%$, the beam intensity is $\sim 3 \cdot 10^6$ per 1.9 sec U-70 spill. A schematic view of the ISTRA+ setup is shown in Fig. 2. The beam particles are deflected by the magnet M_1 and are measured by four proportional chambers BPC_1—BPC_4 with 1 mm wire spacing, the kaon identification is done by three threshold Cerenkov counters $\check{C}_0$—$\check{C}_2$. The 9 meter long vacuum decay volume is surrounded by eight lead glass rings used to veto low energy photons. The 72-cell lead-glass calorimeter SP_2 plays the same role. The decay products are deflected in the magnet M_2 with 1 Tm field integral and are measured with 2 mm step proportional chambers PC_1—PC_3, with 1 cm cell drift chambers DC_1—DC_3 and, finally, with 2 cm diameter drift tubes DT_1—DT_4. The wide aperture threshold Cerenkov counters $\check{C}_3$,$\check{C}_4$, filled with He, serve to trigger electrons and are not used in the present measurement. SP_1 is a 576-cell lead-glass calorimeter, followed by HC, a scintillator-iron sampling hadron calorimeter. MH is a 11x11 cell scintillating hodoscope, used to improve the time resolution of the tracking system, MuH is a 7x7 cell muon hodoscope.

The trigger is provided by scintillation counters S_1—S_5, beam Cerenkov counters and by the analog sum of amplitudes from last dynodes of the SP_1 : T=$S_1 \cdot S_2 \cdot S_3 \cdot \overline{S}_4 \cdot \check{C}_1 \cdot \overline{\check{C}}_2 \cdot \overline{\check{C}}_3 \cdot \overline{S}_5 \cdot \Sigma(SP_1)$, here S_4 is a scintillation counter with a hole to suppress the beam halo, S_5 is a counter downstream of

the setup at the beam focus, $\Sigma(\mathrm{SP}_1)$ requires that the analog sum to be larger than the MIP signal.

During the first run in March-April 2001, 363 million of trigger events were recorded. During the second physics run in November-December 2001 350 million trigger events were collected with higher beam intensity and stronger trigger requirements. This information is complemented by about 300 M Monte Carlo (MC) events generated using Geant3 [10] for the dominant K^- decay modes. Signal efficiency for possible sgoldstino production has been estimated using 1.5 M generated events; in this sample the sgoldstino mass m_P is varied from 0 to 200 MeV/c^2 in steps of 10 MeV/c^2. These simulated signal events were weighted using the matrix element given in [2].

Some information on the data processing and reconstruction procedures is given in [7, 8, 9], here we briefly mention the details relevant for $\pi^-\pi^\circ$ + missing energy event selection.

The muon identification (see [8]) is based on the information from the SP_1 and the HC. The electron identification (see [7]) is done using the E/p ratio — the energy of the shower associated with a charged track and the charged track momentum.

A set of cuts is developed to suppress backgrounds to possible sgoldstino production:

0) Events with one reconstructed charged track and with two showers in the calorimeter SP_1 are selected. We require the effective mass $m(\gamma\gamma)$ to be within ± 50 MeV/c^2 from m_{π°. Events with a vertex inside $400 < z < 1650$ cm are selected.

1) "Soft" charged pion identification is applied: tracks identified as electron or muon (as described in [7, 8]) are rejected.

2) Events with missing energy $E_{mis} = E_{beam} - E_{\pi^-} - E_{\pi^\circ}$ above 3 GeV are selected. This cut serves to reduce the $K_{\pi 2}$ contamination. The missing energy spectra for the second run data, MC background and MC signal with m_P =90 MeV/c^2 are compared in Fig. 3.

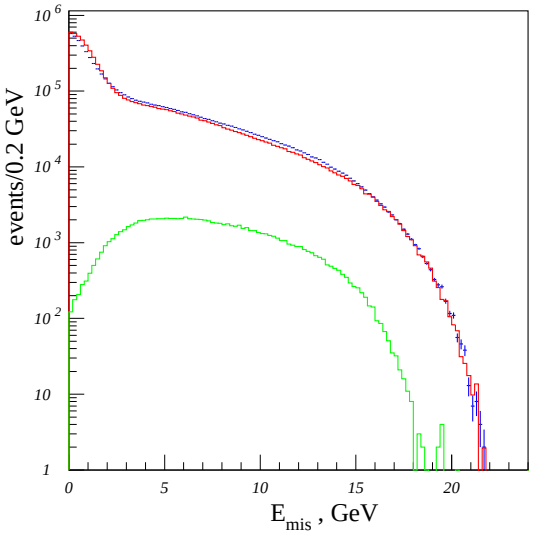

Figure 3: Missing energy spectra, second run data. Points show real data, upper histogram — background MC events, lower histogram — signal MC events for $m_P = 90$ MeV/c^2.

3) To reduce the background caused by secondary charged particles in the photon sample, the MH information is used. The distribution of the distance Δr between an SP_1 shower and the nearest MH hit in the plane transverse to the beam is shown in Fig. 4. An event is selected if at least one shower has Δr greater than 10 cm.

4) The events where one of the photons is suspected to be irradiated by the charged particle in a detector material upstream/inside M2-magnet are rejected. Such photons have nearly the same x coordinate (in the direction of the magnetic field) as the charged track on the SP_1, i.e. an event is rejected if for one or both showers have the difference $\Delta x = |x_{ch} - x_\gamma| < 7$ cm .

5) Events which pass K_{e3} 2C-fit [7] are removed.

6) An additional cut on the charged pion momentum p^* in the kaon rest frame $p^*(\pi^-) < 180$ MeV/c

is applied to suppress the tails from the $K_{\pi 2}$ decay.

7) The pion identification, mainly based on the HC information is required . The efficiency and muon suppression of this selection has been determined using $K_{\mu 2}$ and $K_{\pi 2}$ decays. The efficiency is found to be 70% and 80% for the first and second run data respectively. The remaining muon admixture is equal to 3% and 2%.

8) The events with missing momentum pointing to the SP_1 working aperture are selected in order to suppress $\pi^-\pi^\circ\gamma$ background.

9) The "Veto" cut uses information from the Guard System (GS) and the guard electromagnetic calorimeter (SP_2): absence of signals above noise threshold is required.

The data reduction information for the second run is given in Table 1 and is compared with the MC-background and with the MC-signal for the sgoldstino mass of $m_P = 90$ MeV/c^2. The cut suppression factors w_{i-1}/w_i for the MC data are calculated using the corresponding matrix elements.

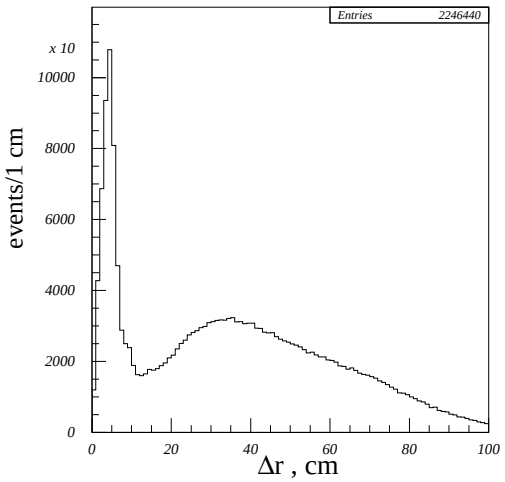

Figure 4: The distance Δr between the SP_1 shower and the nearest MH hit, second run data.

The influence of the last cuts on the missing mass squared spectra $(P_K - P_{\pi^-} - P_{\pi^\circ})^2$ is shown in Fig. 5. The left wide bump in Fig. 5 is due to $K_{\mu 3}$ decays, the shift to the negative missing mass squared is caused by the use of the pion mass in its calculations. The second peak is caused by $\pi^-\pi^\circ(\pi^\circ)$ decays with photons from the second π° escaping detection both in the SP_1 and in the "Veto" system.

3 Analysis and results

As a result of the previous cuts, especially the last "Veto" cut, the π°-signal practically disappears from the $\gamma\gamma$ mass spectrum for certain missing mass (m_P) intervals. To illustrate that, the $m(\gamma\gamma)$ spectrum after cut (2) is shown in Fig. 6 (left half). The right half of Fig. 6 shows the $\gamma\gamma$ mass spectra after the "Veto" cut for several m_P intervals. It is clearly seen that the π° signal survives for the region of the $\pi^-\pi^\circ(\pi^\circ)$ decay only. This situation allows us to perform an effective background subtraction procedure: the $m(\gamma\gamma)$ spectra for 10 MeV/c^2 m_P intervals, starting from $m_P = 0$, are fitted by the sum of a Gaussian (with the fixed width of 9.3 MeV/c^2 and the fixed mass of 135 MeV/c^2) and a quadratic (or linear) polynomial. Such fits are shown in Fig. 6 (right half). Fig.7 shows the obtained numbers of π° (N_{π^0}) plotted in the corresponding missing mass (m_P) bins. A possible constraint $N_{\pi^0} > 0$ is not imposed during the fit, thus N_{π^0} is negative for some bins. This was done to avoid a specialized treatment of asymmetric errors during later analysis. The sgoldstino signal would look like a peak in this "filtered" missing mass spectrum of Fig.7, similar to that of a well seen π^0 peak (at 135 MeV/c^2) from the $K^- \to \pi^-\pi^\circ(\pi^\circ)$ events which pass the "Veto" cut.

Table 1: Event reduction statistics for the 2^{nd} run, the data, the background MC and the signal MC with $m_P = 90$ MeV/c^2.

Cut	data	N_{i-1}/N_i	BG MC	w_{i-1}/w_i	signal MC	w_{i-1}/w_i
0) 1 π^-, $m(\gamma\gamma)$ near $m(\pi^\circ)$	9943046		5512890		98289	
1) no (e, μ)	7771606	1.28	4545059	1.19	93470	1.05
2) E$_{mis} > 3.0$ GeV	1123220	6.92	588735	7.78	82602	1.17
3) MH filter	939052	1.20	516922	1.19	74744	1.09
4) conv. gammas	722622	1.30	426286	1.22	56513	1.25
5) no K_{e3} fit	458338	1.58	201580	2.27	35906	1.69
6) $p^*(\pi^-) < 180$ MeV/c	326935	1.40	134706	1.28	35698	1.01
7) π^- identification	122804	2.66	68380	2.06	33401	1.06
8) $10 < r < 60$ cm	108992	1.13	60698	1.12	31431	1.06
9) Veto	31451	3.47	18674	3.58	31104	1.01

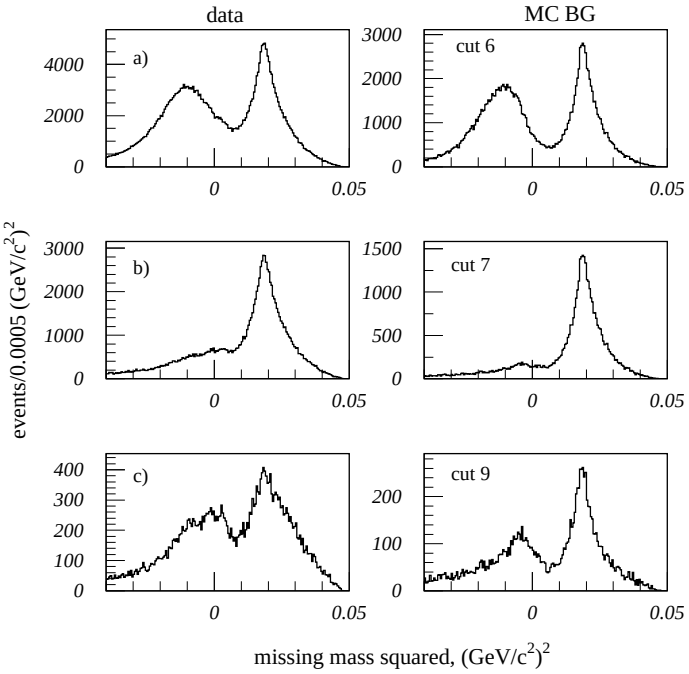

Figure 5: Missing mass squared distributions after cuts 6 (a) , 7 (b) and 9 (c), left column — second run data, right column — MC for dominant K^- decay modes. The bin size is equal to 0.0005 (GeV/c^2)^2.

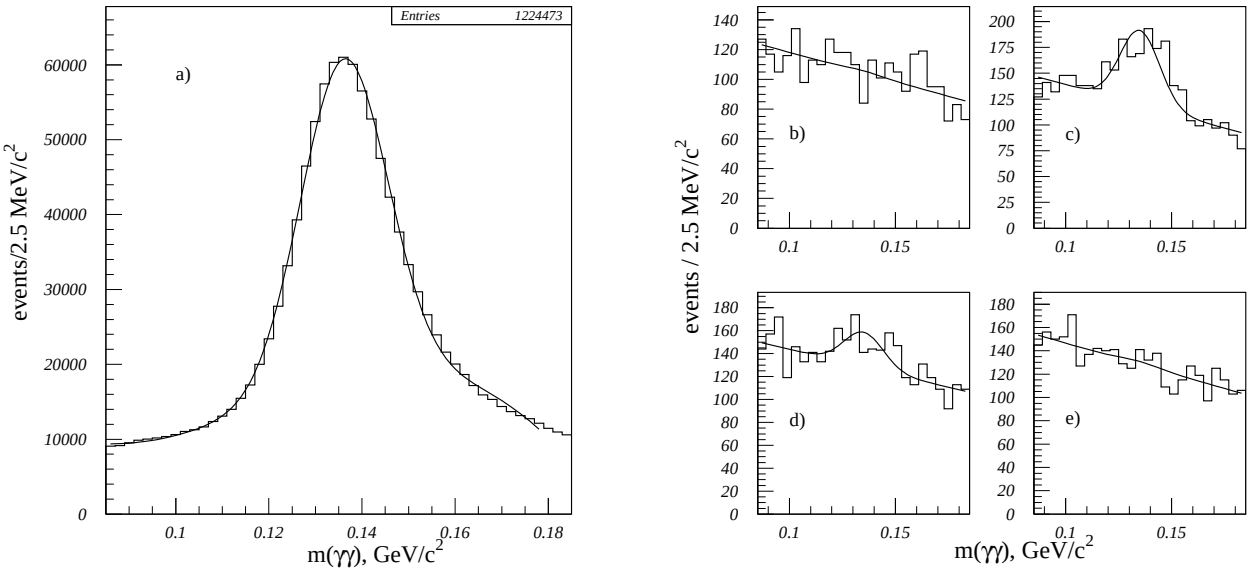

Figure 6: a) $m(\gamma\gamma)$ spectrum for events with $E_{mis} > 3.0$ GeV with the result of the fit by the sum of the Gaussian and a third degree polynomial; $m(\gamma\gamma)$ spectra after the "Veto" cut for the missing mass m_P intervals 120-130(b), 130-140(c), 140-150(d) and 150-160 MeV/c^2(e).

No significant signal is observed. To obtain the upper limits for the number of sgoldstino events at different m_P (N_{sig}), the "filtered" missing mass spectrum is fitted by the sum of the signal Gaussian (with a fixed width of $\sigma = 11.1$ MeV/c^2, as determined from the signal MC) and a background. The background is described by the sum of two components: a Gaussian for the $\pi^-\pi^\circ(\pi^\circ)$ peak plus the constant term. The integral of the signal+background function over a particular bin (-i-) enters into the χ^2 function which is minimized by the "MINUIT" program [11]. Fig.7 shows an example of such a fit with $m_P = 185$ MeV/c^2. To be consistent, we do not impose the constraint $N_{sig} > 0$. We checked that the constrained fit gives comparable or smaller error estimates (corresponding to lower upper limits), i.e. the procedure used is more "conservative". One-sided upper limits for the number of signal events at the 90% confidence level are calculated as

$$N_{UL} = max(N_{sig}, 0) + 1.28 \cdot \sigma \quad , \tag{3}$$

where σ is an error estimate for N_{sig}. The upper limit for the branching ratio (UL) is calculated as

$$UL = \frac{N_{UL} \cdot 0.2116 \cdot \varepsilon(K_{\pi 2})}{N(K_{\pi 2}) \cdot \varepsilon} \tag{4}$$

where 0.2116 is the branching ratio $Br(K_{\pi 2})$, and $N(K_{\pi 2})$ is the number of reconstructed $K^- \to \pi^-\pi^\circ$ decays found to be ~ 1.5 M events for the first and ~ 4.5 M events for the second run. The values ε and $\varepsilon(K_{\pi 2})$ are respective efficiencies for $K^- \to \pi^-\pi^\circ\ P$ and $K_{\pi 2}$ decays, which include both the reconstruction efficiency and geometrical acceptance. To avoid the systematics associated with the

"Veto" cut (cut 9), we have applied it to the selected $K_{\pi 2}$ events. The measured efficiency of this cut is $90\ \%$ and is explained by random signals in the Veto system due to the presence of the beam halo and event overlaps.

Since the Veto inefficiency has the same influence on both the signal and the normalization sample, it cancels out in (4). The signal efficiency ε rises monotonically from $\sim\ 3.3\%$ to $\sim\ 11.3\%$ in the mass interval from 0 to 170 MeV/c^2 and then drops slightly to the value $\sim\ 10.3\%$ at 200 MeV/c^2. This behavior is practically identical for both runs. The $K_{\pi 2}$ efficiency $\varepsilon(K_{\pi 2})$ is equal to $15.8\ \%$ for the first run and $22.4\ \%$ for the second run. The weighted average ratio $\varepsilon/\varepsilon(K_{\pi 2})$ with the weights proportional to the run statistics is used for the combined data sample.

The final results obtained with the combined statistics of two runs are given in Fig. 8. The left part of this figure shows a comparison of our results with that published by the E787 collaboration [3].

The obtained upper limits can be transformed into the limits for the value of the modulus $|h_{12}^D|$ (see equations 1,2). The corresponding limits are compared in Fig. 8 (right part) with the theoretical limit evaluated using $K_L - K_S$ mass difference. A generalization of the formula B9 in the Appendices B of the paper [2] for the non-zero m_P [12] was used when extracting the $|h_{12}^D|$.

The systematics in the upper limits is discussed in the following section.

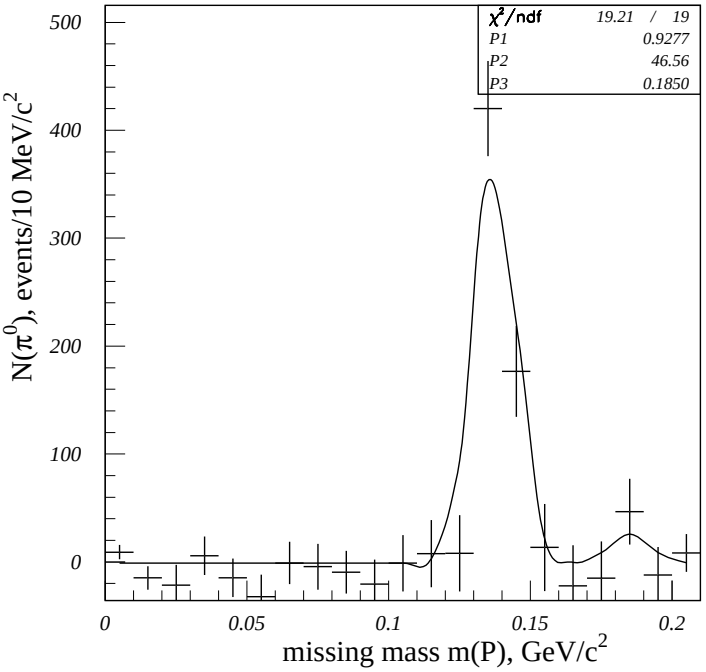

Figure 7: The number of π° from the fit of the $m(\gamma\gamma)$ mass spectra plotted in the corresponding missing mass m_P bins. The curve is the result of the fit with an assumed sgoldstino signal at $m_P = 185$ MeV/c^2 .

4 Systematics

The comparison of our data with the background MC shows some discrepancies: although the total suppression factors of the selection cuts for the data and MC are equal within a few percent, a significant difference of 25-30 $\%$ is observed for cuts 6,7(see Table.1). Some differences seen in Figs 3 and 5 are explained by the non-Gaussian tails (absent in the MC data) of the beam momentum distribution and higher noise levels in the real data.

To estimate the systematics related to the observed differences, we have calculated from our data the well known branching ratio $Br(K^- \to \pi^-\pi^\circ\pi^\circ)$, using the events of this decay with one π°

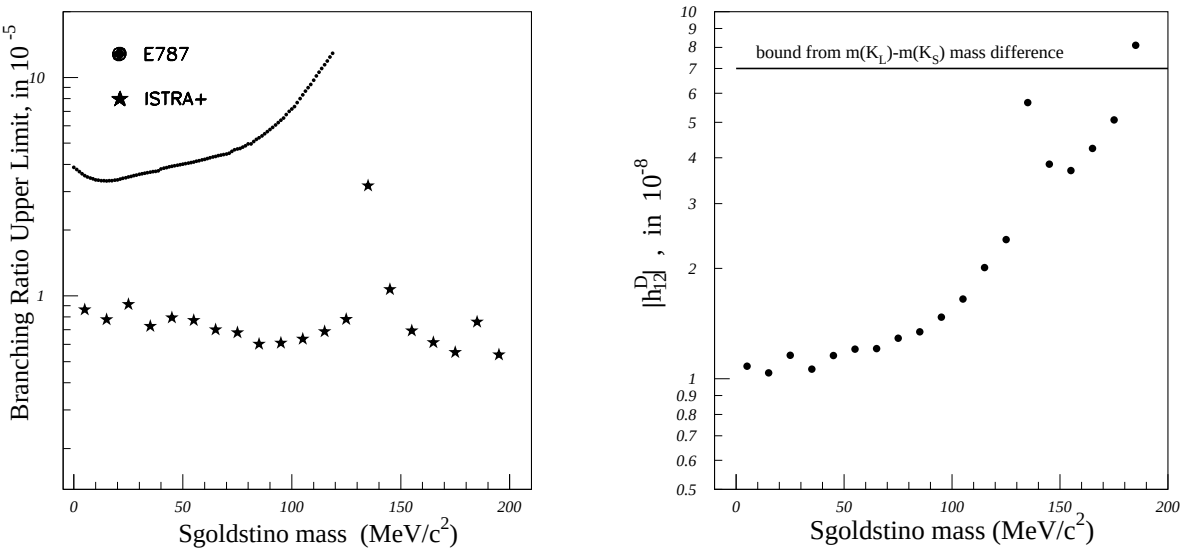

Figure 8: The $90\ \%$ CL upper limit for the $Br(K^- \to \pi^-\pi^\circ P)$ versus sgoldstino mass compared with the E787 upper limit(left), the $90\ \%$ CL upper limit for the $|h_{12}^D|$ compared with the theoretical limit from $K_L - K_S$ mass difference(right).

missed, i.e. events with the topology $K^- \to \pi^-\pi^\circ(\pi^\circ)$. In this test the missing π° plays the role of sgoldstino.

For the test, we have repeated the every step of our analysis, i.e. event selection, which includes: cuts 0-8, filtering of the missing mass spectrum, fitting and normalizing to the $K^- \to \pi^-\pi^\circ$ decay. The only cut which was removed is the "Veto" cut (cut 9) in order not to suppress the escaping π°. The branching ratio $Br(K^- \to \pi^-\pi^\circ\pi^\circ)$ has been measured to be $1.64 \pm 0.03\%$(stat.) compared with the PDG value $1.73 \pm 0.04\ \%$ [13], i.e. the observed systematics is $\sim 5\%$. It has been taken into account by the multiplication of the UL in (4) by the factor of 1.05 for all data points.

This procedure ensures the absence of the systematics in the upper limit for sgoldstino mass $m_P \simeq \mathrm{m}_{\pi^\circ}$. To estimate the residual systematics for other mass bins the upper limits were recalculated for:

a) different cut levels in the cuts 2 — 9;

b) with a different background parametrization for $m(\gamma\gamma)$ (Fig. 6) and N_{π° (Fig. 7) spectra;

c) variation of the theoretical parameters [2] used in the signal Monte-Carlo program.

For each new set of cuts and for each mass point m_P the upper limits were calculated exactly in the same way as for the main set of cuts. The observed variation of the results gives the estimate of the remaining systematics. For example, for $m_P = 95$ MeV/c^2 we got 17%, 11% and 4% variation for the contributions a), b) and c) respectively.

This systematics for each point was taken into account by the corresponding increase (by the summary multiplicative factor) of the upper limits (21% increase for $m_P = 95$ MeV/c^2 equal to sum of the contributions a), b) and c)). For other data points the systematics varies from 16 to 25 %.

5 Summary and conclusions

A search for the light pseudoscalar sgoldstino in the $K^- \to \pi^-\pi^\circ P$ decay is performed. It is assumed that sgoldstinos decay outside the detector. No signal is seen in the m_P mass interval between 0 and 200 MeV/c^2. The upper limits at 90% CL are set to be $\sim 9.0 \cdot 10^{-6}$ for the sgoldstino mass range from 0 to 200 MeV/c^2, excluding the interval near $m(\pi^\circ)$, where the limit is $\sim 3.5 \cdot 10^{-5}$. These results improve the confidence limits published by the E787 collaboration. Our limits improve also the theoretical constraints on $|h_{12}^D|$ from $K_L - K_S$ mass difference.

The authors would like to thank D.S. Gorbunov, V.A. Matveev and V.A. Rubakov, for numerous discussions.

The work is supported in part by the RFBR grants N03-02-16330 (IHEP group) and N03-02-16135 (INR group).

References

[1] G. Giudice and R. Rattazzi, Phys.Rep.**322** (1999) 419; S. Dubrovsky, D. Gorbunov and S. Troitsky, Usp.Fiz.Nauk **169** (1999) 705, English translation in Phys. Usp. **42**(1999) 623 (hep-ph/9905466).

[2] D.S. Gorbunov and V.A. Rubakov, Phys. Rev. **D64** (2001) 054008.

[3] S. Adler et al., E787 Collaboration, Phys. Rev. **D63** (2001) 032004.

[4] L. Littenberg, Rare kaon and pion decays, Lectures given at the PSI Summer School on Particle Physics, Zuoz, 2002, PSI Proceedings 03-02, March 2003, preprint hep-ex/0212005.

[5] V.V. Anisimovsky et al., E949 Collaboration, Phys. Rev. Lett. **93** (2004) 031801.

[6] S. Adler et al., E787 Collaboration, Phys. Rev. **D70** (2004) 037102.

[7] I.V. Ajinenko et al., Phys.Atom.Nucl. 65(2002) 2064; Yad. Fiz. 65(2002)2125.

[8] I.V. Ajinenko et al., Phys.Atom.Nucl. 66(2003) 105; Yad. Fiz. 66(2003) 107.

[9] I.V. Ajinenko et al., Phys. Lett. **B567** (2003) 159.

[10] R. Brun et al, CERN-DD/EE/84-1, CERN, Geneva, 1984.

[11] F. James, MINUIT reference manual, version 94.1, CERN Program Library Long Writeup D506, CERN, Geneva, 1998; F. James, Interpretation of the errors on parameters as given by MINUIT, supplement to long write-up of routine D506, 1978.

[12] D.S. Gorbunov, private communication.

[13] R. Hagiwara et al., Review of Particle Physics, Particle Data Group, Phys. Rev. **D66** (2002) 010001.